

This is a repository copy of *Magnetic domain evolution in permalloy mesoscopic dots*.

White Rose Research Online URL for this paper:

<https://eprints.whiterose.ac.uk/1853/>

Article:

Hirohata, A. orcid.org/0000-0001-9107-2330, Leung, H.T., Xu, Y.B. et al. (4 more authors) (1999) Magnetic domain evolution in permalloy mesoscopic dots. IEEE Transactions on Magnetism. pp. 3886-3888. ISSN 1941-0069

<https://doi.org/10.1109/20.800697>

Reuse

Items deposited in White Rose Research Online are protected by copyright, with all rights reserved unless indicated otherwise. They may be downloaded and/or printed for private study, or other acts as permitted by national copyright laws. The publisher or other rights holders may allow further reproduction and re-use of the full text version. This is indicated by the licence information on the White Rose Research Online record for the item.

Takedown

If you consider content in White Rose Research Online to be in breach of UK law, please notify us by emailing eprints@whiterose.ac.uk including the URL of the record and the reason for the withdrawal request.

Magnetic Domain Evolution in Permalloy Mesoscopic Dots

A. Hirohata, H.T. Leung, Y.B. Xu, C.C. Yao, W.Y. Lee, and J.A.C. Bland
 Cavendish Laboratory, University of Cambridge, Madingley Road, Cambridge CB3 0HE, England

S.N. Holmes

Cambridge Research Laboratory, Toshiba Research Europe Limited
 260 Cambridge Science Park, Milton Road, Cambridge CB4 4WE, England

Abstract—Permalloy ($\text{Ni}_{80}\text{Fe}_{20}$) squares (30 nm thick and $w \mu\text{m}$ wide; $1 \leq w \leq 200 \mu\text{m}$) and circular disks (30 nm thick and $r \mu\text{m}$ diameter; $1 \leq r \leq 200 \mu\text{m}$) prepared on a GaAs (100) substrate were observed in both their demagnetized and remanent states by magnetic force microscopy (MFM) associated with non-contact atomic force microscopy (NC-AFM). The squares ($2 \leq w \mu\text{m}$) exhibited conventional closure domains and the corner plays a very important role in creating new walls. The circular disks, on the other hand, formed either vortex domain ($5 \leq r \leq 20 \mu\text{m}$) or multi-domain ($50 \leq r \mu\text{m}$) states. The magnetization rotation is observed by MFM to change according to the size and shape of the elements. The MFM observations are supported by micromagnetic calculations which confirm the effect of the corner on the domain wall formation.

Index Terms—Mesoscopic structures, magnetic force microscopy, micromagnetic calculation, magnetic domain evolution.

I. INTRODUCTION

A great deal of attention has been paid to artificially fabricated mesoscopic magnetic structures [1]–[7]. Square [1], [2], [4]–[6] and circular dots [3], [7] provide especially good examples because of their potential for various kinds of applications in magnetoelectronics and devices [8]. Arrays of mesoscopic dots are also relevant for macroscopic measurements of microscopic behavior such as quantum tunneling [9]. In such array structures, however, it is very difficult to avoid magnetic interactions with the neighboring structures. To clarify the magnetic domain configurations in a single structure, a well separated set of mesoscopic dots should be examined.

The domain configuration is determined by the competition among various contributions to the free energy [10]. For instance, it has been reported that the uniaxial anisotropy has an important role in giving rise to magnetic domains in Fe (001) square elements [4]. To highlight shape effects, a low anisotropy material is appropriate.

In this study, in order to concentrate on the size and shape effects on domain formation we fabricated a wide size range of permalloy ($\text{Ni}_{80}\text{Fe}_{20}$) small squares (30 nm thick and $w \mu\text{m}$ wide; $1 \leq w \leq 200 \mu\text{m}$) and circular disks (30 nm thick and $r \mu\text{m}$ diameter; $1 \leq r \leq 200 \mu\text{m}$) prepared on a GaAs (100) substrate. Scanning probe microscopy (SPM, Digital Instruments, Nanoscope III) was used to reveal the role of both the size and shape of the structures in the formation of domain walls, and this was supported by micromagnetic calculations.

II. EXPERIMENTAL PROCEDURE

Manuscript received March 5, 1999.
 A. Hirohata, 44-1223-337006, fax 44-1223-337333, ah242@cam.ac.uk,
http://homer.phy.cam.ac.uk/TFM_Home.html; J.A.C. Bland, 44-1223-337436, fax 44-1223-350266, jacb1@phy.cam.ac.uk.

A 3 nm Au/30 nm $\text{Ni}_{80}\text{Fe}_{20}$ continuous film structure was deposited on a GaAs (100) substrate in ultrahigh vacuum (UHV). The permalloy layers were deposited at a rate of 0.25 nm/min. The pressure during the growth was 5.0×10^{-9} Torr, while the substrate was held at 300 K. The film was then annealed at 400 K for 30 minutes to remove the uniaxial anisotropy induced during the growth. The permalloy elements of variable size ($1 \leq w, r \leq 200 \mu\text{m}$) were fabricated by electron beam lithography and optimized pattern transfer techniques based on a combination of both dry and wet etching.

The permalloy structures were observed in both their demagnetized and remanent states by magnetic force microscopy (MFM) together with non-contact magnetic force microscopy (NC-AFM). A commercial Si probe (Digital Instruments, Pointprobe magnetic force sensor MESP) coated with CoCr was used and the distance between probe and sample was set as 5 nm for NC-AFM tapping mode and 100 nm for MFM measurement [11]. The tip of this probe was magnetized before each observation. The magnetic probe typically has a spring constant of 2.8 N/m and a resonance frequency of 75 kHz. The resolving power of these two forms of microscopy was approximately 10 nm for NC-AFM and 100 nm for MFM, respectively.

III. RESULTS AND DISCUSSION

With squares, we found three classes of magnetic domain structure in the demagnetized states as shown in Fig. 1: (a) a single domain at $w=1 \mu\text{m}$, (b) a four-wall closure domain structure in the range of $2 \leq w \leq 5 \mu\text{m}$ and (c) complex domain structures with the formation of new domains from one corner ($10 \leq w \mu\text{m}$). Figure 1(b), for example, shows both MFM

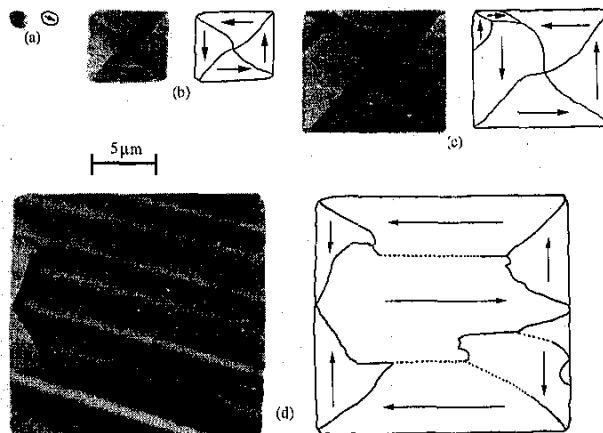


Fig. 1. MFM images and corresponding schematic magnetic domain configurations of permalloy squares of the size $w =$ (a) 1 μm , (b) 5 μm , (c) 10 μm , and (d) 20 μm . Artificial effects caused by the surroundings are also seen on these pictures as periodical lines. For the 1 μm square, significant rounding of the element shape occurs due to the patterning process.

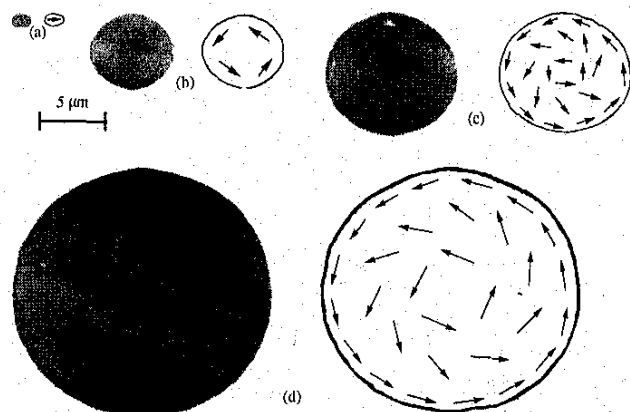


Fig. 2. MFM images and corresponding schematic magnetic domain configurations of permalloy circular disks of the size $r =$ (a) 1 μm , (b) 5 μm , (c) 10 μm and (d) 20 μm .

images and schematic domain configurations of the permalloy square of $w = 5 \mu\text{m}$ and a typical closure domain can be seen as expected [1], [12]. It should be noted that the domain wall is not straight, which suggests that the magnetization in this sample has a rotating component. From the results for square elements with $w = 10 \mu\text{m}$, new magnetic domains appear from the corners of the squares and provide new complex closure domain structures (see Fig. 1(c)). With increased w , the nucleation of new domains is found to occur from the corners, reducing the magnetostatic energy in the samples. Since this also occurs in their remanent states, it can be inferred that the domain walls connected with the corners are energetically stable.

Comparing Fig. 1(b) and (c), the non-straight walls are found at the corners of the squares, while the straight ones are seen in the middle. This result suggests that the magnetization is aligned at the corners parallel to the edges due to the reduction of the magnetostatic energy at the edges. In the larger size samples, these rotation regions are negligible compared with the length of the straight walls.

Figure 2 shows the domain evolution with diameter in the case of circular disks in the demagnetized states. The first stage is (a) a single domain ($1 \leq r \leq 2 \mu\text{m}$). At the next stage, circular vortex domain structures are observed ($5 \leq r \leq 20 \mu\text{m}$) as shown in Fig. 2(b)-(d), since the permalloy samples have no crystal-induced anisotropy. The larger diameter samples finally show complex domain structures with walls ($50 \leq w \mu\text{m}$) [13]. In the remanent states, however, since one particular magnetization direction is enhanced by the applied magnetic field direction in plane, circular dots with small diameter ($10 \leq r \leq 20 \mu\text{m}$) also exhibit several domain walls.

Comparing the results for these two shapes, we conclude that the magnetization in a certain size of particles tends to rotate in order to reduce the exchange energy in the demagnetized states. However, in the presence of a corner, the domain configuration is mainly determined by the competition between the exchange field and the demagnetizing field. When an external magnetic field is applied, one particular magnetization direction parallel to the field is enhanced. As a result, domains with the magnetization direction parallel to the field direction expand in size. Such a tendency, as well as domain wall nucleation for favorably aligned domains, can also be observed in the remanent states. We found that the wall nucleation is dependent on both the field direction and the presence of the corners, suggesting that the corners play a very important role in the wall nucleation.

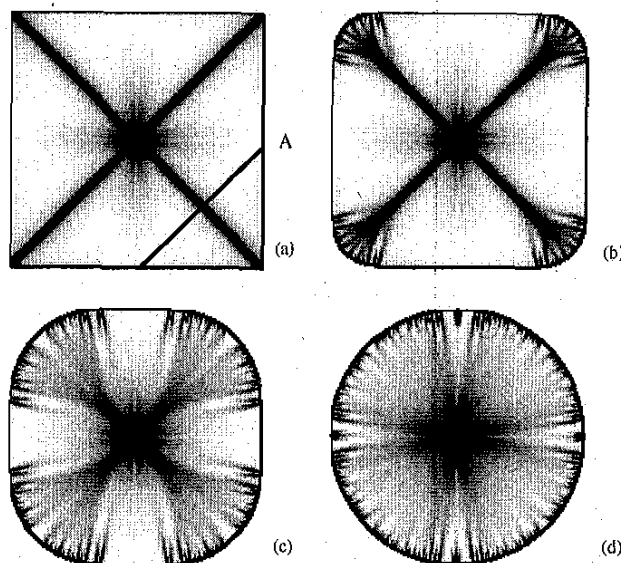


Fig. 3. Micromagnetic simulations for (a) a permalloy square ($w = 5 \mu\text{m}$) and (d) a circular disk ($r = 5 \mu\text{m}$) together with several intermediate states: a square with rounded corners $r_c =$ (b) 0.9 μm and (c) 1.8 μm . Black lines connected with the corners correspond to magnetic domain walls.

IV. NUMERICAL CALCULATIONS

A micromagnetic numerical calculation was carried out to confirm the critical point for domain wall formation using a *finite difference method*. The system was divided into 30 cubic cells. The demagnetization field, magnetic anisotropy field and the exchange field were calculated at the position of each cell which was assumed to possess a constant magnitude of magnetization M_s . The magnetization was assumed to point in any direction. M_s was randomly aligned at the first stage and each magnetization rotated in the direction such as to reduce the total energy at the position. The total energy of the samples was also calculated and the stable domain configuration was defined at the minimum energy.

The results of numerical simulations are shown in Fig. 3. In these pictures, the magnitude of the gradient of the magnetization is shown by the gray scale. Since the magnetization in the domain walls is rapidly rotating, the walls are shown as black lines, corresponding to a high gradient value. The results for the 5 μm square and circular disk for example are almost the same as the MFM images as shown in Fig. 3(a) and (d), respectively. In order to determine the existence of the rotating magnetization components, we also calculated the domain configurations of rounded squares, in which each corner was shaped as a quarter circle. The domain configurations of these intermediate structures are also shown in Fig. 3(b) and (c). It should be noted that the black lines become wider with increasing diameter of the rounded corners r_c . This means that the domain wall width increases with r_c , suggesting that the walls are stable anywhere within the dark lines. The width near the corner, especially, increases dramatically, which supports the observation of rotating domain walls using MFM (see Fig. 1(b)).

Figure 4 shows the calculated domain wall width w_d in the middle of the closure domain walls (cross-section A in Fig. 3(a)) in the 5 μm square dots with the rounded corners ($0 \leq r_c \leq 2.5 \mu\text{m}$). The straight walls from the center to the middle are stable in this area, while the regions in which the magnetization rotates significantly appear at the corners. At $r_c = 0$, the wall width of the square is calculated to be around 200 nm, when the wall width is defined by the magnetization rotation angle of 45° . The

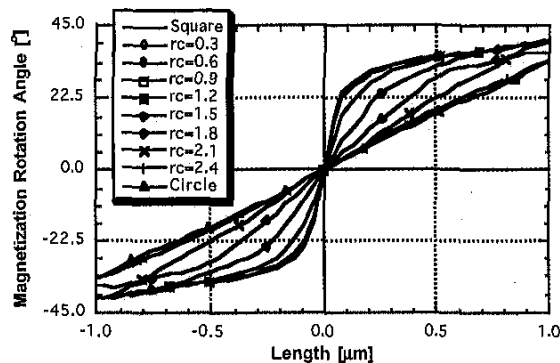


Fig. 4. Numerically calculated domain wall width for rounded squares different radius r_c and also the circular disks and fully square elements.

simulated value is almost double that found in bulk permalloy [14]. It should be noted that the wall width in the rounded squares ($0 \leq r_c \leq 0.9 \mu\text{m}$) is almost the same as that in the square. The width w_d increases rapidly with r_c , suggesting that the walls can be observed at anywhere within the corner region. This supports the observation of curved walls by MFM (see Figs. 1(b) and (c)).

V. CONCLUSION

We investigated the domain configurations in a wide size range of permalloy ($\text{Ni}_{80}\text{Fe}_{20}$) small squares (30 nm thick and $w \mu\text{m}$ wide; $1 \leq w \leq 200 \mu\text{m}$) and circular disks (30 nm thick and $r \mu\text{m}$ diameter; $1 \leq r \leq 200 \mu\text{m}$) prepared on a GaAs (100) substrate in both their demagnetized and remanent states using MFM. The squares ($2 \leq w \mu\text{m}$) exhibited conventional closure domains and new walls were formed from the corner. The circular disks, on the other hand, create either vortex domain ($5 \leq r \leq 20 \mu\text{m}$) or multi-domain ($50 \leq r \mu\text{m}$) configurations. From these results, the magnetization in a certain element size was found to rotate due to the competition between the exchange and the magnetostatic field. The corners of the squares have a role in both the nucleation of new domain walls and the stabilization of the walls. Using micromagnetic calculations, the effect of the definition of the corner on domain wall formation was assessed. The observed evolution in the domain structures in changing shape from square to circular elements is supported by the

results of the micromagnetic simulations.

ACKNOWLEDGMENT

AH would like to express his appreciation to Toshiba Research Europe Limited, Cambridge Overseas Trust and Selwyn College (Cambridge) for their financial support. We acknowledge the support of the EPSRC and EU (SUBMAGDEV and MASSDOTS).

REFERENCES

- [1] K. Runge, Y. Nozaki, Y. Otani, H. Miyajima, B. Pannetier, T. Matsuda, and A. Tonomura, "High-resolution observation of magnetization processes in $2 \mu\text{m} \times 2 \mu\text{m} \times 0.04 \mu\text{m}$ permalloy particles," *J. Appl. Phys.*, vol. 79, pp. 5075-5077, April 1996.
- [2] D. A. Herman, Jr., B.E. Argyle, and B. Petek, "Bloch lines, cross ties, and taffy in permalloy," *J. Appl. Phys.*, vol. 61, pp. 4200-4206, April 1987.
- [3] C. Miramond, C. Fermon, F. Rousseaux, D. Decanini, and F. Carcenac, "Permalloy cylindrical submicron size dot arrays," *J. Magn. Magn. Mater.*, vol. 165, pp. 500-503, 1997.
- [4] E. Gu, E. Ahmad, S.J. Gray, C. Daboo, J.A.C. Bland, L.M. Brown, M. Rührig, A.J. McGibbon, and J.N. Chapman, "Micromagnetism of epitaxial $\text{Fe}(001)$ elements on the mesoscale," *Phys. Rev. Lett.*, vol. 78, pp. 1158-1161, February 1997.
- [5] S. Gider, J. Shi, D.D. Awschalom, P.D. Hopkins, K.L. Campman, A.C. Gossard, A.D. Kent, and S. von Molnár, "Imaging and magnetometry of switching in nanometer-scale iron particles," *Appl. Phys. Lett.*, vol. 69, pp. 3269-3271, November 1996.
- [6] H. Hehn, K. Ounadjela, S. Padovani, J.P. Bucher, J. Arabski, N. Bardou, B. Bartenlian, C. Chapert, F. Rousseaux, D. Decanini, F. Carcenac, E. Cambri, and M.F. Ravet, "Structural and magnetic study of submicronic single crystal cobalt box arrays," *J. Appl. Phys.*, vol. 79, pp. 5068-5070, April 1996.
- [7] A. Fernandez, M.R. Gibbons, M.A. Wall, and C.J. Cerjan, "Magnetic domain structure and magnetization reversal in submicron-scale Co dots," *J. Magn. Magn. Mater.*, vol. 190, pp. 71-80, December 1998.
- [8] M. Johnson, "Spin-polarization of gold films via transport," *J. Appl. Phys.*, vol. 75, pp. 6714-6719, May 1994.
- [9] C. Paulsen, L.C. Sampaio, R.T. Tachouères, B. Barbara, D. Fruchart, A. Marchand, J.L. Tholence, and M. Uehara, "Mesoscopic quantum tunneling in small ferromagnetic particles," *J. Magn. Magn. Mater.*, vol. 116, pp. 67-69, 1992.
- [10] W.F. Brown, Jr., *Micromagnetics*. New York: Wiley, 1963, pp. 1.
- [11] K. Babcock, V. Elings, M. Dugas, and S. Loper, "Optimization of thin-film tips for magnetic force microscopy," *IEEE Trans. Magn.*, vol. 30, pp. 4503-4505, November 1994; K.L. Babcock, V.B. Elings, J. Shi, D.D. Awschalom, and M. Dugas, "Field-dependence of microscopic probes in magnetic force microscopy," *Appl. Phys. Lett.*, vol. 69, pp. 705-707, July 1996.
- [12] R.P. Cowburn and M.E. Welland, "Phase transitions in planar magnetic nanostructures," *Appl. Phys. Lett.*, vol. 72, pp. 2041-2043, April 1998.
- [13] W.Y. Lee, B.-Ch. Choi, J. Lee, C.C. Yao, Y.B. Xu, D.G. Hasko, and J.A.C. Bland, "Dynamic scaling of magnetic hysteresis in micron-sized $\text{Ni}_{80}\text{Fe}_{20}$ discs," *Appl. Phys. Lett.*, vol. 74, pp. 1609-1611, March 1999.
- [14] S. Chikazumi, *Physics of Magnetism*. Oxford: Clarendon, 1997, pp. 407.